



# Experimental test of an innovative high concentration nanofluid solar collector



Gianpiero Colangelo<sup>\*</sup>, Ernani Favale, Paola Miglietta, Arturo de Risi, Marco Milanese, Domenico Laforgia

Dipartimento di Ingegneria dell'Innovazione, Università del Salento, Via per Arnesano, 73100 Lecce, Italy

## HIGHLIGHTS

- A new type of nanofluid thermal solar collector has been built and tested.
- $\text{Al}_2\text{O}_3$ -distilled water based nanofluid at high concentration has been used.
- Experimental results showed an increase of thermal efficiency up to 11.7%.

## ARTICLE INFO

### Article history:

Received 30 January 2015

Received in revised form 17 April 2015

Accepted 10 May 2015

Available online 9 June 2015

### Keywords:

Nanofluid

$\text{Al}_2\text{O}_3$

Sedimentation

Flat panel solar thermal collector

Convective heat transfer coefficient

## ABSTRACT

In this study, a modified flat panel solar thermal collector was built and thermal efficiency was measured with two heat transfer fluids: distilled water and  $\text{Al}_2\text{O}_3$ -distilled water based nanofluid at high concentration (3.0%) volume fraction of solid phase. In this work for the first time nanofluid with high nanoparticle concentration has been used thanks to a modified solar thermal collector, based on patent WO2011138752 A1, which consists in bottom and top headers properly shaped in order to reduce sedimentation of clusters of nanoparticles. Thermal efficiency has been measured through an experimental setup, according to EN 12975-2 standard. Experimental results showed that an increase of thermal efficiency up to 11.7% compared to that measured with water has been obtained by using nanofluid. Besides effect of nanofluid on thermal efficiency is greater at high temperatures.

© 2015 Elsevier Ltd. All rights reserved.

## 1. Introduction

The interest in improving heat transfer capability of heat transfer fluids have been growing in the last decade and particular attention has been given to nanofluids, a biphasic suspension of metal or metal oxide nanoparticles in a traditional heat transfer fluid such as water, oil, ethylene glycol [1] etc. Therefore nanofluids can also be applied in energy systems in order to increase their efficiency [2] or to enhance heat transfer coefficients in heat exchangers [3], as in cooling system for wind turbines proposed by de Risi et al. [4]. Thermal conductivity of nanofluids and convective heat transfer coefficient have been investigated for different materials and particle sizes by many authors [5]. Syam Sundar et al. [6] analyzed water and ethylene glycol mixture inseminated with  $\text{Al}_2\text{O}_3$  nanoparticles. They obtained a thermal conductivity enhancement from 9.8% to 17.89% for  $\text{Al}_2\text{O}_3$  nanofluid with 0.8 vol% of solid phase, in a range of temperature between 15 °C and 50 °C. Yiamsawas et al. [7] measured thermal conductivity

of water based nanofluids with  $\text{Al}_2\text{O}_3$  nanoparticles, with volume fraction from 0.0% to 8.0%, in a temperature range between 15 °C and 65 °C. They obtained an increase between 2% and 20%. Minsta et al. [8] measured thermal conductivity of water based nanofluids with  $\text{Al}_2\text{O}_3$  nanoparticles with an average dimension of 47 nm and 37 nm respectively. An enhancement up to 30.0%, in a range of volume fraction from 1.0% to 18.0% was found.  $\text{Al}_2\text{O}_3$ -water based nanofluids at a volume fraction of 1.0%, 2.0% and 3.0% have been prepared and their thermal conductivity has been measured at 20 °C by Colangelo et al. [9]. It was observed an enhancement up to 6.70%.

Although nanoparticles are more stable in base fluid compared with larger particles, which yield problems of clogging, abrasion and sedimentation [10,11], viscosity of nanofluid is higher than that of base fluid.

Convective heat transfer coefficient of nanofluids has been also investigated by many authors. Heyhat et al. [12] measured heat transfer coefficient of water based nanofluids with  $\text{Al}_2\text{O}_3$  nanoparticles with an average diameter of 40.0 nm and a volume fraction from 0.1% to 2.0% in a circular tube, with constant wall temperature under turbulent flow conditions. Results were compared with

<sup>\*</sup> Corresponding author. Tel.: +39 0832297752; fax: +39 0832297777.

E-mail address: [gianpiero.colangelo@unisalento.it](mailto:gianpiero.colangelo@unisalento.it) (G. Colangelo).

## Nomenclature

$v_h$	inlet average velocity (m/s)	$A_a$	aperture area of the collector (m <sup>2</sup> )
$A_h$	inlet cross section area (m <sup>2</sup> )	$T_m$	reduced temperature difference (°Cm <sup>2</sup> /W)
$A_i$	cross section area at $i$ position ( $i = 1, 2, \dots, 7$ ) (m <sup>2</sup> )	$U_{Tout}$	uncertainty for outlet temperature (%)
$\dot{m}_i$	mass flowrate at $i$ position ( $i = 1, 2, \dots, 7$ ) (kg/s)	$U_{Tin}$	uncertainty for inlet temperature (%)
$G$	global solar irradiance (W/m <sup>2</sup> )	$U_G$	uncertainty for solar radiation (%)
$T_a$	surrounding air temperature (°C)	$U_\eta$	uncertainty for efficiency (%)
$G_d/G$	diffuse fraction (%)	$a_1$	heat transfer coefficient (W/m <sup>2</sup> °C)
$u$	surrounding air speed (m/s)	$R^2$	uncertainty coefficient
$T_{in}$	collector inlet temperature (°C)		
$T_{out}$	collector outlet temperature (°C)		
$Q$	power extracted by solar collector (W)		
$c_p$	specific heat (J/kg K)		
$T_m$	mean temperature (°C)		
$\dot{m}_h$	mass flowrate (kg/s)		
$A_A$	absorber area of the collector (m <sup>2</sup> )		

## Greek symbols

$\Theta$	incidence angle of beam irradiance (°)
$\eta$	efficiency
$\eta_0$	zero loss efficiency
$\rho$	density of the fluid (kg/m <sup>3</sup> )

convective heat transfer coefficient obtained with base fluid. An enhancement up to 23.0% was obtained. Hwang et al. [13] studied the convective heat transfer coefficient of water–Al<sub>2</sub>O<sub>3</sub> nanofluids flowing in a stainless steel tube. The nanoparticles had an average diameter of 30 nm and they obtained an increase up to 8.0% at a concentration of solid phase of 0.3%. An increase of 20.0% and 15.0% of convective heat transfer coefficient, under laminar and turbulent flow conditions respectively, with a volume fraction of 3.0% in a stainless steel tube with an inner diameter of 4.57 mm, was obtained by Kim et al. [14].

Fotukian and Esfahany [15] experimentally investigated that the maximum value of heat transfer coefficient enhancement is 48% for alumina nanofluids, with a volume fraction less than 0.2%, compared to water, in turbulent flow condition, inside a copper tube with inner diameter of 5.0 mm. Besides Wen and Ding [16] found that the trend of convective heat coefficient for Al<sub>2</sub>O<sub>3</sub> nanofluids (with a volume concentration from 0.6% to 1.6%) is a function of volume fraction and that in the entry region the enhancement is much higher and then it decreases with axial distance. Heris et al. [17] obtained enhancement of heat transfer coefficient up to 20.0% compared to that of the water with alumina nanofluids with a volume fraction from 0.2% to 2.5%. Heris et al. [18] observed that heat transfer coefficient of alumina nanofluids increases of 29.0%, under laminar flow condition, with a volume fraction of 2.5%. Anoop et al. [19] studied the effect of nanoparticles size on heat transfer coefficient of Al<sub>2</sub>O<sub>3</sub>–water based nanofluids. An enhancement of 25% for 45 nm nanoparticles and 11% for 150 nm ones at 4 wt% has been obtained. Sahin et al. [20] determined heat transfer coefficient of Al<sub>2</sub>O<sub>3</sub>–water nanofluids (from 0.5 vol% to 4.0 vol%) in an aluminum circular tube, with inner diameter of 11.7 mm, under a constant heat flux. A parabolic trend was obtained and maximum values were measured at 1.0 vol% of solid phase.

Nanofluids can be employed in solar energy systems in order to improve their efficiency. Taylor et al. [21] asserted that nanofluids in a receiver of a concentrating solar thermal system can increase efficiency up to 10%. Otanicar et al. [22] investigated the effect of water based nanofluids on a micro scale direct absorption solar collector (DASC). Using silver nanoparticles, CNTs and graphite nanoparticles respectively an enhancement of the efficiency with a volume fraction of 0.5% was obtained. Besides a remarkable efficiency dependence on particle size was observed for silver nanoparticles with a diameter between 20 nm and 40 nm. Yousefi et al. [23] investigated nanofluids effect in a flat plate solar collector using water–Al<sub>2</sub>O<sub>3</sub> dispersion at a weight fraction of 0.2%.

An enhancement of 28.3% in comparison with water was obtained and adding a surfactant to the suspension the efficiency enhanced of 15.63%. Chaji et al. [24] studied the effect of TiO<sub>2</sub> water based nanofluid inside a small flat plate solar collector with 0.1, 0.2 and 0.3 wt% of solid phase. An index of collector total efficiency was used to compare the different cases. Efficiency was investigated at 36 l/m<sup>2</sup> h, 72 l/m<sup>2</sup> h, and 108 l/m<sup>2</sup> h respectively. An enhancement between 2.6% and 7.0% was obtained. Moghadam et al. [25] studied the effect of CuO–water base nanofluid at 0.4 vol% and average diameter of 40 nm on the efficiency of a flat plate solar collector. An enhancement of 4.74% and 21.8% compared to that of water has been obtained with a mass flow rate of 2 and 1 kg/min respectively.

Although nanoparticles are more stable in liquid phase than millimeter or micrometer particles, sedimentation phenomenon can be detected in piping of the systems and therefore also in solar collector, as Colangelo et al. [26] demonstrated with a water–Al<sub>2</sub>O<sub>3</sub> nanofluid with a volume fraction between 1.0% and 3.0%. They proposed a modified flat plate solar collector to avoid this phenomenon, in order to maintain a constant flow velocity along both bottom and top header. The sedimentation analysis was carried out through an optical investigation. For this purpose, a modified flat plate solar collector was built with transparent tubes.

The aim of this work is to continue the research on a modified flat plate solar collector analyzed by Colangelo et al. [26] and to evaluate the increase of performance of a flat plate solar collector due to the use of water–Al<sub>2</sub>O<sub>3</sub> nanofluid as heat transfer fluid. In particular, a modified flat plate solar collector using water–Al<sub>2</sub>O<sub>3</sub> nanofluids was built and its efficiency was measured under different working conditions, according to EN 12975-2 standard. In this work for the first time the performance of a nanofluid solar collector is evaluated according to EN 12975-2 standard [27]. In other works the experimental campaign has been carried out using a traditional solar collector with no compliance to any standard. In this work, instead, a new model of solar collector has been designed and built, able to work specifically with nanofluids and all the experimental tests have been carried out following the EN 12975-2 standard. In this way the comparison between the heat transfer fluids has been performed in controlled and standard conditions, reducing the possibility of error. In this work a volume fraction of 3.0% of nanoparticles has been chosen to evaluate the possible problems related to sedimentation and to collect data about the most stressing conditions for the system. Other works used lower nanoparticle concentrations [22–25] to avoid inevitable sedimentation problems and to reduce pumping problems. In this

work, for the first time, it was possible to obtain experimental data using high nanoparticles concentration, due to the peculiar design of the header tubes of the new solar collector, studied on purpose, that is able to avoid sedimentation problems, that are present in traditional solar collectors and that make impossible to carry out such experiments with high nanoparticle concentration.

## 2. Nanofluid preparation

Commercial  $\text{Al}_2\text{O}_3$  nanoparticles and distilled water were used to prepare nanofluid with a volume fraction of 3.0% of nanoparticles, which have spherical shape, density of  $3700 \text{ kg/m}^3$  and average diameter of 45 nm. No dispersant was used. The suspension was mixed with a magnetic stirrer at 700 rpm for 60 min and vibrated in an ultrasonic bath at 59 kHz and 285 W for 180 min to break the nanoparticles cluster to improve stability. Finally a second mixing with magnetic stirrer was made.

$\text{Al}_2\text{O}_3$  nanoparticles have been chosen because they are more stable in water and cheaper than other materials. Therefore they are a good compromise considering stability, costs and thermo-physical properties of nanofluids [26]. Stability of nanofluid was investigated with Turbiscan LabExpert. It consists in a detection head that moves along a cylindrical cell, where the nanofluid sample is placed. The detection head has a near infrared light source ( $\lambda = 800 \text{ nm}$ ) and two detectors that receive the light transmitted through the sample and the backscattered light respectively. The backscattering variation value is directly proportional to the variation of particles concentration at every position along the cell. Stability of the suspension was measured for 2 h at  $25^\circ\text{C}$  and Fig. 1 shows backscattering during measurement. Only at the bottom of the cell a delta backscattering of 7.5% was measured, while in other positions this variation is negligible. This means that a little part of solid phase is sedimented (very large cluster nanoparticles that ultrasonic bath was not able to reduce), while the remaining solid phase is stable in the suspension.

Average cluster size of the solid phase of nanofluid was measured using DLS technique (Zetasizer Nano – S – Malvern Instruments). Three measurements have been made and the mean value was calculated. An average diameter of 128.2 nm has been obtained, as shown in Fig. 2.

Thermal conductivity of water and water– $\text{Al}_2\text{O}_3$  3.0 vol% nanofluid was measured through hot-wire technique, according to ASTM D 2717-95 standard. Water thermal conductivity was  $0.606 \pm 0.006 \text{ W/m}^\circ\text{C}$  and an enhancement of 6.5% was obtained with nanofluid ( $0.645 \pm 0.006 \text{ W/m}^\circ\text{C}$ ) at  $20^\circ\text{C}$ .

## 3. Flat panel solar thermal collector

An innovative flat panel solar thermal collector, working with nanofluid, was designed and built. For both top and bottom header, copper tubes with inner diameter of 20.0 mm and thickness of 1.0 mm respectively were used, while copper tubes with inner

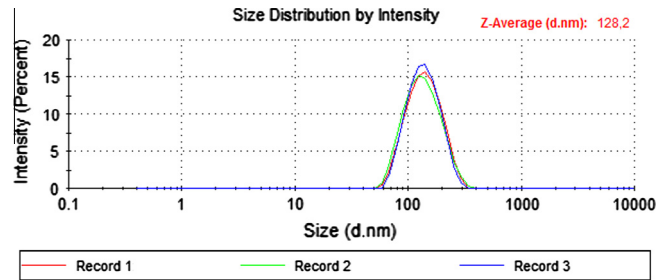


Fig. 2. Cluster dimension of  $\text{Al}_2\text{O}_3$  water based nanofluid at 3 vol%.

diameter of 10.0 mm and thickness of 1.0 mm respectively were employed for riser tubes. The tubes were fixed on a  $1332 \times 860 \text{ mm}$  copper plate through thermal adhesive. Tubes and copper plate, called absorber, were coated with a black paint (Fig. 3).

The absorber was inserted inside a galvanized steel frame, covered with a polycarbonate plate and insulated with a glass wool mattress and polyurethane panel (Fig. 4).

A copper wedge shaped element was inserted inside the top and bottom header to maintain a constant flow velocity in order to avoid sedimentation phenomenon. In fact, as Fig. 5 shows, in a traditional flat panel solar thermal collector, inside the bottom header flow rate decreases because the fluid is distributed to the riser tubes. Similarly, inside top header flow rate increases because heat transfer fluid comes out from the riser tubes.

These variations of velocity yield sedimentation phenomenon of solid phase along both top and bottom header. In particular the amount of precipitated material is inversely proportional to the mean velocity on the cross section, as explained in [26]. Therefore through a shaped element it is possible to vary the cross section along longitudinal axis in order to maintain a constant velocity. Referring to Fig. 5,  $\dot{m}_h$  is the mass flow rate at the inlet of the bottom header:

$$\dot{m}_h = \rho v_h A_h \quad (1)$$

where  $\rho$  ( $\text{kg/m}^3$ ) is the density of the heat transfer fluid,  $v_h$  ( $\text{m/s}$ ) is the average velocity at the inlet cross section and  $A_h$  ( $\text{m}^2$ ) is the cross section area. For each cross section, in order to maintain a constant velocity, it is possible to write mass flow rate as:

$$\dot{m}_i = \rho v_h A_i \quad (i = 1, 2, \dots, 7) \quad (2)$$

therefore

$$A_i = \frac{\dot{m}_i}{\rho v_h} \quad (i = 1, 2, \dots, 7) \quad (3)$$

Flat panel solar thermal collector used in this investigation has eight riser tubes. Considering an uniform distribution of the fluid to all riser tubes,  $\dot{m}_i$  can be calculated through the following equation:

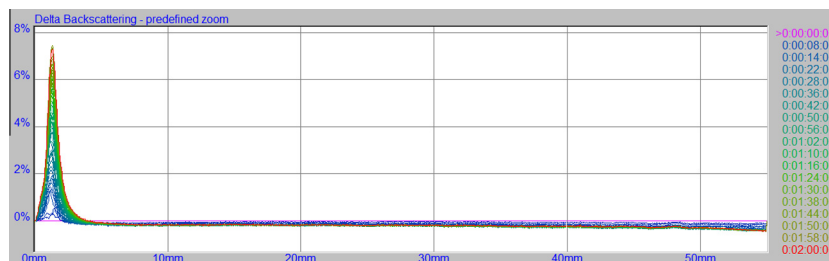


Fig. 1. Delta backscattering measurement of  $\text{Al}_2\text{O}_3$  water based nanofluid at 3 vol%.

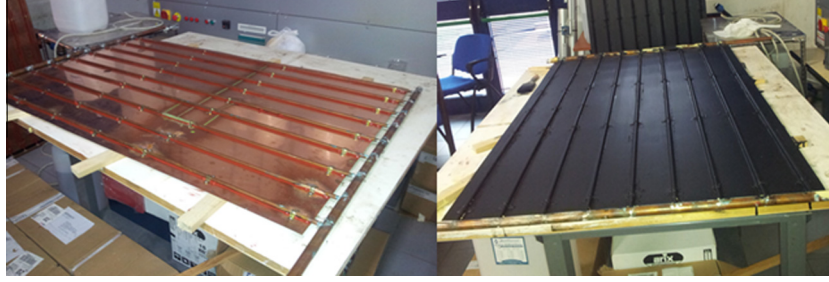


Fig. 3. Tubes and copper plate fixed and coated with black paint (Absorber).

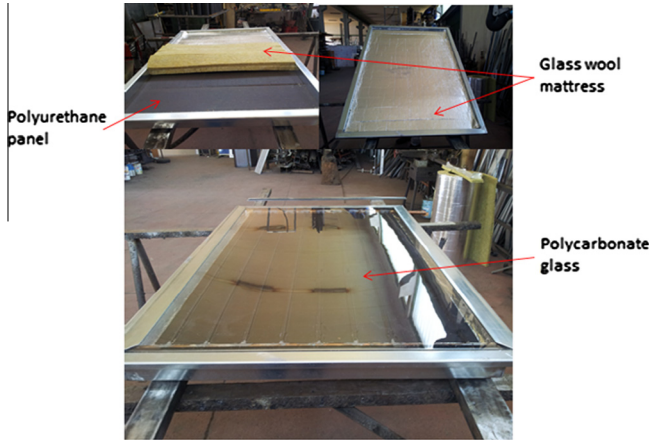


Fig. 4. Flat panel solar thermal collector.

$$\dot{m}_i = \dot{m}_h \left( 1 - \frac{i}{8} \right) \quad (i = 1, 2, \dots, 7) \quad (4)$$

Substituting Eqs. (1) and (4) in Eq. (2),  $A_i$  can be written as:

$$A_i = A_h \left( 1 - \frac{i}{8} \right) \quad (i = 1, 2, \dots, 7) \quad (5)$$

A generic cross section,  $A_i$ , along bottom header is a circular segment of area:

$$A_i = \frac{r^2}{2} \left( \frac{\alpha_i \pi}{180} - \sin \alpha_i \right) = A_h \left( 1 - \frac{i}{8} \right) \quad (i = 1, 2, \dots, 7) \quad (6)$$

where  $\alpha_i$  is the central angle in degrees and  $r$  is the inner radius. It is possible to obtain  $\alpha_i$  from Eq. (6), for example  $\alpha_7 = 3.925 \cdot 10^{-5} \text{ m}^2$

and  $\alpha_7 \approx 101^\circ$ . Shaped element inserted in both top and bottom header guarantees that in each cross section area is less than or equal to  $A_i$ .

Besides, in every cross section, velocity has a vertical component from the bottom to the top that yields a mixing between liquid and solid phase that enhances mixing of the suspension (Patent WO2011138752 A1).

Fig. 6 shows the top header (or bottom header) with the shaped element.

#### 4. Experimental setup

The experimental setup to measure efficiency of flat panel solar thermal collector was based on EN 12975-2 standard and is schematically shown in Fig. 7. The experimental tests of the solar collector were carried out at University of Salento in Lecce, Italy (latitude is  $40^\circ 20' 04.5'' \text{N}$  and longitude is  $18^\circ 06' 47.5'' \text{E}$ ). In a closed hydraulic circuit with expansion tank (9), heat transfer fluid flows by means of a pump (13). The system has a solenoid valve (11) on a bypass to adjust flow rate of heat transfer fluid and a safety valve (8) to protect the system from overpressure. Flow rate is measured by a Coriolis flow meter, Micro Motion® series F025S (5). If possible, efficiency measurements shall be made over a temperature range between ambient temperature and  $80^\circ \text{C}$ , under clear sky conditions [27]. For this purpose inlet temperature of solar collector is adjusted by band heaters (12) controlled by a PID circuit. Thermal equilibrium is guaranteed by a shell and tube heat exchanger (14) and an air–water heat exchanger (15). 4-Wire Pt100 sensors (6) are used to measure both inlet and outlet temperature of solar collector and heat exchanger. Pt100 were arranged at no more than 200 mm from both the collector inlet and outlet. Another Pt100 (6a) is used by PID circuit of band heaters. The system has two pyranometers (LP PYRA 02, Delta Ohm

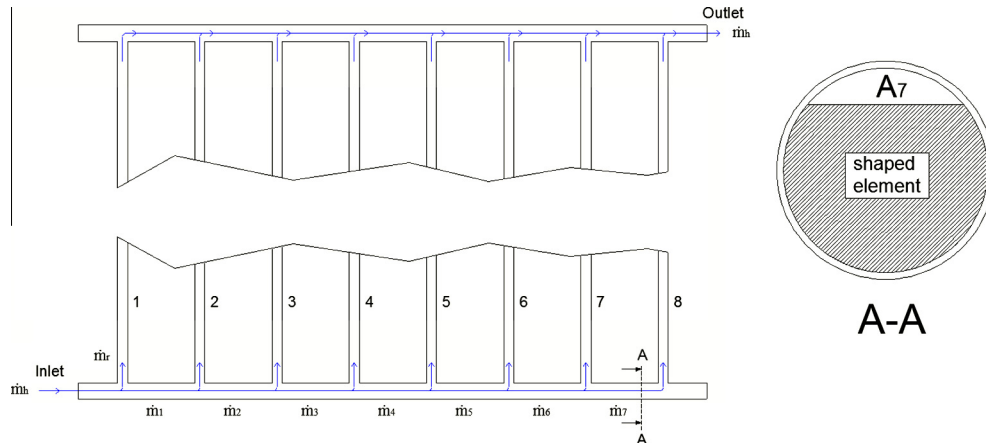


Fig. 5. Flow in a traditional flat panel solar thermal collector.



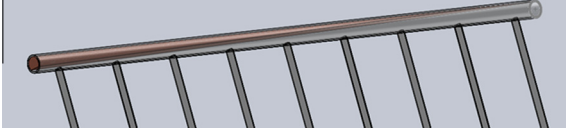


Fig. 6. Top header (or bottom header) with modified internal shaped element.

srl). The first one (2) measures direct irradiance on solar collector. The second one (3) is employed to measure diffuse irradiance. An anemometer (4) and a thermometer (17) measure wind velocity and air temperature respectively. Finally a radial ventilator is placed to guarantee a constant air speed over the collector (16) (see Fig. 8).

A steady-state method is used to calculate solar collector's efficiency, according to EN 12975-2 standard. The test conditions are shown in Table 1 [27,28].

The power extracted by solar collector,  $\dot{Q}$ , is calculated with Eq. (7):

$$\dot{Q} = \dot{m}_h c_p (T_{out} - T_{in}) \quad (7)$$

where  $c_p$  is the specific heat of the fluid at mean temperature, calculated with Eq. (8):

$$T_m = \frac{T_{out} + T_{in}}{2} \quad (8)$$

and ( $\dot{m}_h$ ) is the mass flowrate.  $\dot{Q}$  can also be obtained through efficiency,  $\eta$  (Eq. (9)):

$$\dot{Q} = AG\eta \quad (9)$$

where  $A$  can be referred to the absorber area ( $A_A$ ) or to the aperture area of the collector ( $A_a$ ).

The instantaneous efficiency is calculated by statistical curve fitting, using the least squares method as in Eq. (10) [27]:

$$\eta = \eta_0 - a_1 T_m^* - a_2 G (T_m^*)^2 \quad (10)$$

where  $\eta_0$  is the zero loss efficiency and  $T_m^*$  is the reduced temperature difference as defined in Eq. (11):

$$T_m^* = \frac{T_m - T_a}{G} \quad (11)$$

In Eq. (10) a second order fit shall not be used if the value of  $a_2$  is negative. In these conditions efficiency can be calculated with Eq. (12):

$$\eta = \eta_0 - a_1 T_m^* = \eta_0 - a_1 \left( \frac{T_m - T_a}{G} \right) \quad (12)$$

$\eta$  is calculated through Eq. (9) and Eq. (10) as described in Eq. (13):

$$\eta = \frac{\dot{Q}}{AG} = \frac{\dot{m}_h c_p (T_{out} - T_{in})}{AG} \quad (13)$$

Therefore  $\eta$  depends on  $\dot{m}$ ,  $T_{out}$ ,  $T_{in}$  and  $G$ . Mass flow rate was measured with an uncertainty  $U_{\dot{m}} < 1.0\%$ . Uncertainties for outlet and inlet temperatures,  $U_{T_{out}}$  and  $U_{T_{in}}$ , were less than  $0.1^\circ\text{C}$ . Finally solar radiation was measured with an uncertainty  $U_G < 2.0\%$ . Table 2 summarizes these uncertainties.

Complex uncertainty,  $U_\eta$ , was calculated with Eq. (14) and was between 0.90% and 5.76%.

$$U_\eta = \sqrt{\left( \frac{\partial \eta}{\partial \dot{m}_h} U_{\dot{m}} \right)^2 + \left( \frac{\partial \eta}{\partial G} U_G \right)^2 + \left( \frac{\partial \eta}{\partial T_{out}} U_{T_{out}} \right)^2 + \left( \frac{\partial \eta}{\partial T_{in}} U_{T_{in}} \right)^2} \quad (14)$$

## 5. Results and discussion

Efficiency of thermal solar collector was investigated with distilled water- $\text{Al}_2\text{O}_3$  nanofluid at a concentration of 0% and 3.0 vol%. This volume fraction of solid phase was chosen on the basis of the experimental investigation carried out by Colangelo et al. [26], regarding heat transfer coefficient of alumina water based nanofluid, prepared with the same materials used in this work.

The values of mass flowrate were close to those used to investigate sedimentation of nanofluid inside solar collector with transparent tubes [26]. Flow rate variation was less than 10.0% from one test period to another one, as required by EN 12975-2 standard.

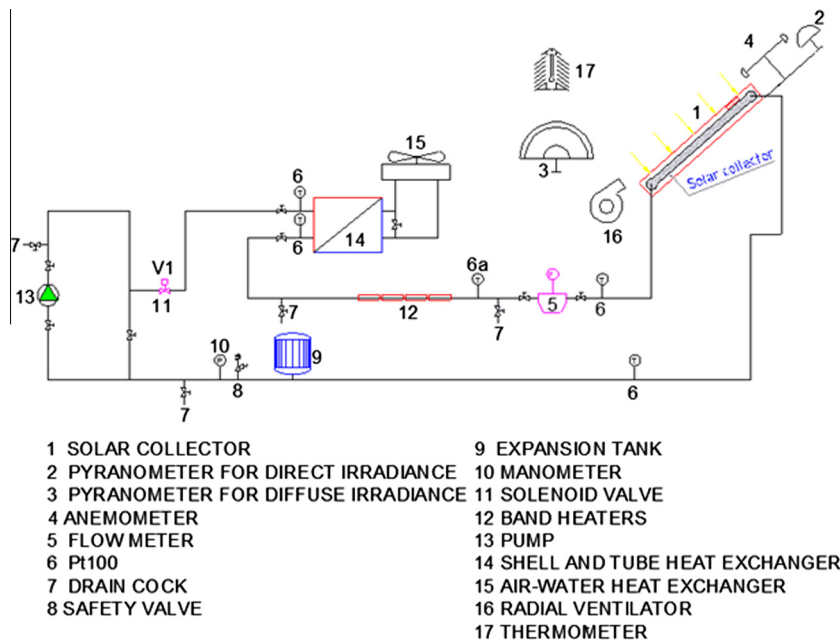


Fig. 7. Layout of experimental setup.

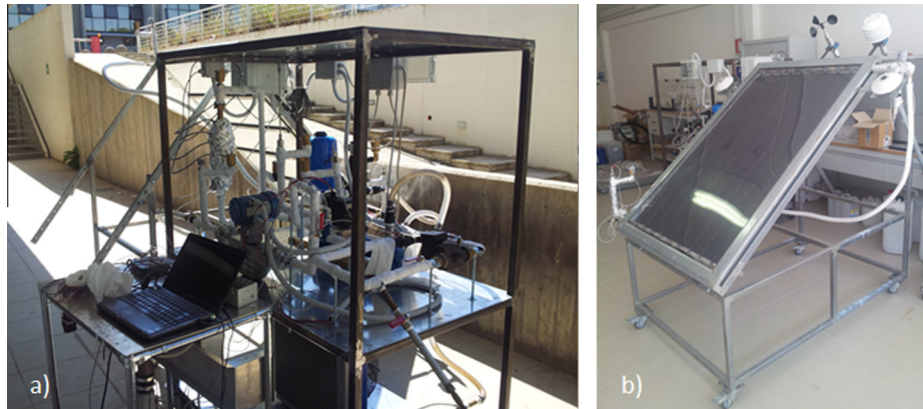


Fig. 8. (a) Experimental setup and (b) flat panel solar thermal collector.

Table 1

Test conditions and deviation.

Parameter	Value	Deviation
Global solar irradiance $G$ ( $\text{W}/\text{m}^2$ )	>700	$\pm 50$
Incidence angle of beam irradiance $\theta$ ( $^\circ$ )	<20	–
Surrounding air temperature $t_a$ ( $^\circ\text{C}$ )	–	$\pm 1$
Diffuse fraction $G_d/G$ (%)	<30	–
Surrounding air speed $u$ (m/s)	3	$\pm 1$
Collector inlet temperature $t_{in}$ ( $^\circ\text{C}$ )	–	$\pm 0.1$

Table 2

Measurement uncertainties.

	Uncertainty
Mass flow rate $\dot{m}$	<1.0%
Outlet temperature $T_{out}$	<0.1 $^\circ\text{C}$
Inlet temperature $T_{in}$	<0.1 $^\circ\text{C}$
Solar radiation $G$	<2.0%

Thermal efficiency analysis of solar collector, with water and nanofluid, was carried out by testing at various reduced temperature difference,  $T_m^*$ , and in several months of the year, as shown in Tables 3 and 4.

Testing procedure consists in measuring parameters needed to calculate efficiency of thermal solar collector at a fixed inlet temperature, which is controlled by the PID circuit. A pre-conditioning period, larger than 15 min, is necessary before measurement period starts. Measurement time must be not less than 10 min, as required by EN 12975-2 standard. Tables 3 and 4. show experimental results for both distilled water and  $\text{Al}_2\text{O}_3$ -distilled water nanofluid 3.0 vol%. With distilled water, the highest efficiency value, 0.4921, has been obtained with a  $T_m^*$  of 0.00958  $^\circ\text{C m}^2/\text{W}$ , which corresponds to an inlet temperature of 30.62  $^\circ\text{C}$ , an ambient temperature of 24.34  $^\circ\text{C}$  and a solar irradiance of 987.63  $\text{W}/\text{m}^2$ . Instead at  $T_m^*$  of 0.04121  $^\circ\text{C m}^2/\text{W}$  the lowest efficiency value has been obtained, 0.3285. In this case inlet temperature, ambient temperature and solar irradiance were 66.35  $^\circ\text{C}$ , 33.59  $^\circ\text{C}$  and 840.78  $\text{W}/\text{m}^2$  respectively.

By using nanofluid as heat transfer fluid the highest efficiency value, 0.5412, has been obtained at inlet temperature of 37.09  $^\circ\text{C}$ , ambient temperature of 33.37  $^\circ\text{C}$  and solar irradiance of 849.06  $\text{W}/\text{m}^2$ . At these conditions  $T_m^*$  is 0.00804. The lowest efficiency, 0.4570, was obtained at  $T_m^*$  = 0.04099  $^\circ\text{C m}^2/\text{W}$  for inlet temperature of 64.31  $^\circ\text{C}$ , ambient temperature of 32.60  $^\circ\text{C}$  and solar irradiance of 839.88  $\text{W}/\text{m}^2$ .

Therefore, the better results have been obtained using  $\text{Al}_2\text{O}_3$ -water nanofluid, in the investigated reduced temperature

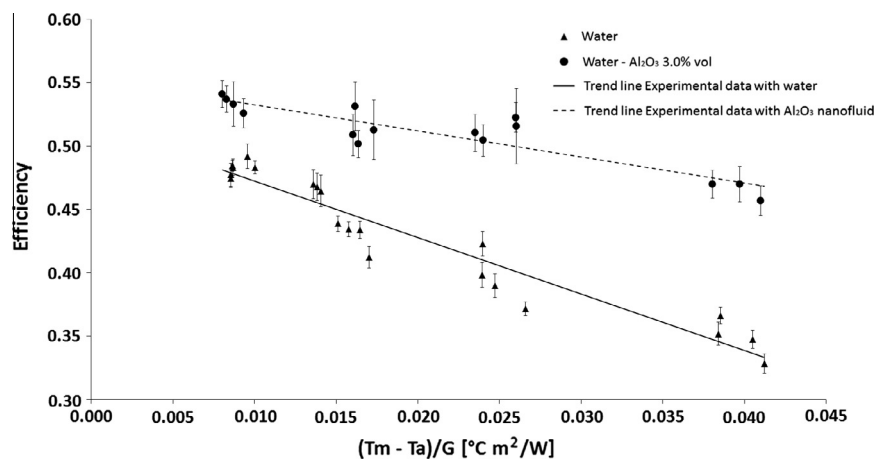
Table 3

Experimental results for bi-distilled water.

Test number	$T_m^*$ ( $^\circ\text{C m}^2/\text{W}$ )	$T_a$ ( $^\circ\text{C}$ )	$G$ ( $\text{W}/\text{m}^2$ )	$\dot{m}$ (kg/s)	$T_{out}$ ( $^\circ\text{C}$ )	$T_{in}$ ( $^\circ\text{C}$ )	$\eta$	$U_\eta$ (%)
1	0.00855	32.11	916.49	0.020231	42.82	37.07	0.4747	0.69
2	0.00855	32.30	899.79	0.020162	42.84	37.14	0.4775	0.60
3	0.00866	22.87	972.21	0.020921	34.30	28.27	0.4847	0.71
4	0.00869	23.12	963.17	0.020986	34.46	28.52	0.4834	0.76
5	0.00958	24.34	987.63	0.020408	36.99	30.62	0.4921	1.49
6	0.01004	22.62	942.69	0.020791	35.02	29.16	0.4832	0.89
7	0.01359	24.20	973.14	0.019727	40.55	34.31	0.4700	0.62
8	0.01384	24.78	980.84	0.019674	41.47	35.23	0.4679	0.77
9	0.01406	25.27	956.42	0.020185	41.68	35.75	0.4646	0.76
10	0.01512	34.29	820.82	0.019447	49.17	44.21	0.4389	1.05
11	0.01576	34.11	801.80	0.019145	49.18	44.31	0.4346	1.04
12	0.01646	33.65	846.06	0.019662	50.07	45.07	0.4340	0.94
13	0.01702	33.17	889.95	0.019990	50.63	45.72	0.4123	1.07
14	0.02393	22.35	943.73	0.020203	47.42	42.44	0.3984	1.23
15	0.02396	24.56	941.32	0.021162	49.62	44.59	0.4229	1.42
16	0.02471	22.26	914.83	0.020125	47.24	42.49	0.3899	1.05
17	0.02659	33.44	867.68	0.019960	58.67	54.34	0.3718	1.01
18	0.03839	33.76	879.95	0.019960	69.62	65.47	0.3520	2.41
19	0.03852	33.53	896.66	0.019344	70.33	65.79	0.3663	1.47
20	0.04051	33.43	864.14	0.019645	70.44	66.41	0.3475	1.74
21	0.04121	33.59	840.78	0.019592	70.12	66.35	0.3285	2.04

**Table 4**Experimental results for Al<sub>2</sub>O<sub>3</sub>–bi-distilled water nanofluid 3.0 vol%.

Test number	$T_m^*$ (°C m <sup>2</sup> /W)	$T_a$ (°C)	$G$ (W/m <sup>2</sup> )	$\dot{m}$ (kg/s)	$T_{out}$ (°C)	$T_{in}$ (°C)	$\eta$	$U_\eta$ (%)
1	<b>0.00804</b>	33.37	849.06	0.020342	43.29	37.09	<b>0.5412</b>	0.91
2	<b>0.00829</b>	33.08	895.36	0.021403	43.58	37.42	<b>0.5372</b>	1.03
3	<b>0.00871</b>	25.61	919.29	0.019972	36.86	30.36	<b>0.5153</b>	3.30
4	<b>0.00934</b>	25.43	917.48	0.020061	37.29	30.69	<b>0.5260</b>	2.20
5	<b>0.01604</b>	35.54	873.83	0.021350	52.41	46.70	<b>0.5089</b>	1.10
6	<b>0.01616</b>	28.79	921.98	0.019736	46.86	40.05	<b>0.5314</b>	2.85
7	<b>0.01636</b>	33.68	895.45	0.021614	51.18	45.48	<b>0.5018</b>	0.79
8	<b>0.01731</b>	33.59	847.80	0.021028	51.10	45.43	<b>0.5130</b>	2.24
9	<b>0.02351</b>	33.11	917.59	0.022700	57.51	51.85	<b>0.5106</b>	2.12
10	<b>0.02401</b>	32.74	912.74	0.020898	57.60	51.70	<b>0.5046</b>	1.20
11	<b>0.02601</b>	34.77	895.39	0.021015	61.11	55.01	<b>0.5227</b>	0.72
12	<b>0.02604</b>	29.72	944.86	0.020847	57.53	51.12	<b>0.5159</b>	1.56
13	<b>0.03805</b>	32.59	896.30	0.019328	69.67	63.70	<b>0.4700</b>	1.94
14	<b>0.03971</b>	32.45	868.34	0.019772	69.76	64.10	<b>0.4699</b>	2.61
15	<b>0.04099</b>	32.60	839.88	0.019650	69.67	64.31	<b>0.4570</b>	2.12

**Fig. 9.** Thermal efficiency of solar collector with water (mass flow rate  $0.02 \pm 0.0008$  kg/s) and Al<sub>2</sub>O<sub>3</sub>–bi-distilled water 3.0 vol% (mass flow rate  $0.02 \pm 0.0015$  kg/s).**Table 5**Values of the zero loss collector efficiency  $\eta_0$ , the heat transfer coefficient  $a_1$  and the uncertainty coefficient  $R^2$ .

Working fluid	$\eta_0$	$a_1$ (W/m <sup>2</sup> °C)	$R^2$
Water	0.517	4.452	0.925
Al <sub>2</sub> O <sub>3</sub> –water nanofluid 3.0 vol%	0.553	2.053	0.819

difference range. Nanoparticles yield an enhancement of thermo-physical properties due to interactions between liquid and solid phases. For example one of these can be the ballistic phonon transport when particles distance is very small [29]. This phenomenon is inversely proportional to the particle size, where the ballistic phonons initiates and persists in the liquid reaching another particle, because the phonon free path is shorter in the liquid than in the solid. This happens if the separation between particles is comparable with liquid layer around the particle. For other authors Brownian motion enhances heat transfer inside suspensions due to collision between liquid molecules and solid particles [30]. Also in this case effect of Brownian motion is inversely proportional to the particle size. These heat transfer mechanisms determine an increase of thermal conductivity of nanofluid compared to that of liquid phase. By using nanofluids convective heat transfer coefficient enhancement is also obtained and it is greater than that of thermal conductivity. For example with Al<sub>2</sub>O<sub>3</sub> nanoparticles at 3 vol%  $T_m^*$  thermal conductivity increases of 6.7% compared to bidistilled water only. At the same volume fraction, heat transfer coefficient of Al<sub>2</sub>O<sub>3</sub> nanofluids is increased up to 25% [26]. For all

these reasons thermal efficiency of solar collector increases by using nanofluids. In fact, random movement of solid phase flattens temperature distribution on cross section of the tubes and increases temperature gradient between fluid and inner surface of the riser tubes. Therefore an enhancement of heat transfer is obtained [26,31]. A comparison on the graph is shown in Fig. 9. It is possible to note that for values of  $T_m^*$  around  $0.0088$  °C m<sup>2</sup>/W, efficiency of solar collector with water is between 0.4747 and 0.4912, while with nanofluid it is between 0.5153 and 0.5412. Therefore, the average efficiency measured in this range of  $T_m^*$  is 0.4826 and 0.5299 for water and nanofluid respectively. The difference between these average efficiencies is about 4.7%. Similarly, around  $0.01579$  °C m<sup>2</sup>/W the average efficiency measured is 0.4460 for water and 0.5137 for nanofluid, with a difference of 6.8%. A difference of average efficiencies of 11.7% has been obtained around  $0.02487$  °C m<sup>2</sup>/W, as well as at  $0.03962$  °C m<sup>2</sup>/W. In fact, observing the trend lines of experimental results, it is possible to note that not only the thermal efficiency of solar collector with nanofluid is higher than that with distilled water for each reduced temperature difference, but the trend line obtained with nanofluid has a slope lower than water only.

Table 5 indicates  $\eta_0$ ,  $a_1$  and  $R^2$  values for instantaneous efficiency according to the Eq. (12). An increase of about 7.0% of the zero loss collector efficiency,  $\eta_0$  ( $\eta$  at  $T_m^* = 0$ ), has been obtained by using nanofluid (from 0.517, for water, to 0.553 for nanofluid), as well as  $a_1$  changes from 4.452 W/m °C to 2.053 W/m °C.

Therefore, the following experimental equations of efficiency of thermal solar collector for water and nanofluid are obtained:

$$\eta_{\text{water}} = 0.517 - 4.452T_m^* \quad (15)$$

and

$$\eta_{\text{nf}} = 0.553 - 2.053T_m^* \quad (16)$$

## 6. Conclusions

A modified flat panel solar thermal collector, to avoid sedimentation of solid phase, was built and an experimental comparison of thermal efficiency between two heat transfer fluids ( $\text{Al}_2\text{O}_3$ -distilled water based nanofluid, at 3% in volume fraction, and distilled water), working in the same thermal solar collector, has been performed. Due to its capability of drastically reducing nanofluid sedimentation inside the tubes, this solar collector made possible, for the first time, to carry out experiments with high nanoparticle concentration.

The modification of the new solar collector consists in a wedge shaped element inserted in both top header and bottom header in order to maintain a constant velocity along longitudinal axial, because amount of precipitated material, in a cross section, is inversely proportional to mean velocity. Efficiency was calculated at various reduced temperature difference,  $T_m^*$ , to which correspond different solar irradiance and inlet temperature in the solar collector. In particular, with distilled water, thermal efficiency was between 0.4921 and 0.3285 for  $T_m^*$  between 0.00855 and 0.04121. By using  $\text{Al}_2\text{O}_3$ -water based nanofluid, thermal efficiency of solar collector was between 0.5412 and 0.4570 for  $T_m^*$  between 0.00804 and 0.04099. Therefore, nanofluid increases efficiency of flat panel solar thermal collector. Besides, from the experimental results, it has been observed that the zero loss collector efficiency  $\eta_0$  of solar thermal collector with  $\text{Al}_2\text{O}_3$ -distilled water based nanofluid is 7% higher than that with distilled water. Finally, the slope of trend line of efficiency with nanofluid is lower than that with water. Therefore, nanofluid is more effective at high temperature.

## Acknowledgements

This work was supported by the SOLAR project (DM19447), funded by the Italian Ministry of University and Research (MIUR).

## References

- [1] Xuan Y, Li Q. Heat transfer enhancement of nanofluids. *Int J Heat Transfer Fluid Flow* 2000;21:58–64.
- [2] Mahian O, Kianifar A, Kalogirou SA, Pop I, Wongwises S. A review of the applications of nanofluids in solar energy. *Int J Heat Mass Trans* 2013;57:582–94.
- [3] Kulkarni Devatta P, Das Debendra K, Vajjha Ravikanth S. Application of nanofluids in heating buildings and reducing pollution. *Appl Energy* 2009;86:2566–73.
- [4] de Risi A, Milanese M, Colangelo G, Laforgia D. High efficiency nanofluid cooling system for wind turbines. *Thermal Sci* 2014;18(2):543–54.
- [5] Lomascolo M, Colangelo G, Milanese M, de Risi A. Review of heat transfer in nanofluids: conductive, convective and radiative experimental results. *Renew Sustain Energy Rev* 2015;43:1182–98.
- [6] Syam Sundar L, Hashim Farooky Md, Naga Sarada S, Singh MK. Experimental thermal conductivity of ethylene glycol and water mixture based low volume concentration of  $\text{Al}_2\text{O}_3$  and  $\text{CuO}$  nanofluids. *Int Commun Heat Mass Transfer* 2013;41:41–6.
- [7] Yiamsawasd T, Dalkilic AS, Wongwises S. Measurement of thermal conductivity of titania and alumina nanofluids. *Thermochim Acta* 2012;545:48–56.
- [8] Minsta HA, Roy G, Nguyen CT, Doucet D. New temperature dependent thermal conductivity data for water-based nanofluids. *Int J Therm Sci* 2009;48:363–71.
- [9] Colangelo G, Favale E, de Risi A, Laforgia D. Results of experimental investigations on the heat conductivity of nanofluids based on diathermic oil for high temperature applications. *Appl Energy* 2012;97:828–33.
- [10] Yurong H, Yi J, Haisheng C, Yulong D, Daqiang C, Huilin L. Heat transfer and flow behavior of aqueous of  $\text{TiO}_2$  nanoparticles (nanofluids) flowing through a vertical pipe. *Int J Heat Mass Transfer* 2007;50:2272–81.
- [11] Nnanna A. Experimental model of temperature-driven nanofluids. *J Heat Transfer* 2007;129:697–704.
- [12] Heyhat MM, Kowsary F, Rashidi AM, Esfehiani SAV, Amrollahi A. Experimental investigation of turbulent flow and convective heat transfer characteristics of alumina water nanofluids in fully developed flow regime. *Int Commun Heat Mass Transfer* 2012;39:1272–8.
- [13] Hwang KS, Jang SP, Choi SUS. Flow and convective heat transfer characteristics of water-based  $\text{Al}_2\text{O}_3$  nanofluids in fully developed laminar flow regime. *Int J Heat Mass Transfer* 2009;52:193–9.
- [14] Kim D, Kwon Y, Cho Y, Li C, Cheong S, Hwang Y. Convective heat transfer characteristics of nanofluids under laminar and turbulent flow conditions. *Curr Appl Phys* 2009;9:119–23.
- [15] Fotukian SM, Esfahany MN. Experimental study of turbulent convective heat transfer and pressure drop of dilute  $\text{CuO}$ /water nanofluid inside a circular tube. *Int Commun Heat Mass Transfer* 2010;37:214–9.
- [16] Wen D, Ding Y. Experimental investigation into convective heat transfer of nanofluids at the entrance region under laminar flow conditions. *Int J Heat Mass Transfer* 2004;47:5181–8.
- [17] Zeinali Heris S, Nasr Esfahany M, Etemad SG. Experimental investigation of convective heat transfer of  $\text{Al}_2\text{O}_3$ /water nanofluid in circular tube. *Int J Heat Fluid Flow* 2007;28:203–10.
- [18] Heris SZ, Etemad SG, Esfahany MN. Experimental investigation of oxide nanofluids laminar flow convective heat transfer. *Int Commun Heat Mass Transfer* 2006;33:529–35.
- [19] Anoop KB, Sundararajan T, Das SK. Effect of particle size on the convective heat transfer in nanofluid in the developing region. *Int J Heat Mass Transfer* 2009;52:2189–95.
- [20] Sahin B, Gültekin GG, Manay E, Karagoz S. Experimental investigation of heat transfer and pressure drop characteristics of  $\text{Al}_2\text{O}_3$ -water nanofluid. *Exp Thermal Fluid Sci* 2013;50:21–8.
- [21] Taylor RA, Phelan PE, Otanicar TP, Tyagi H, Trimble S. 2010. Applicability of nanofluids in concentrated solar energy harvesting. In: *Proceedings of the ASME 2010, 4th International Conference on Energy Sustainability*; 1: p. 825–32.
- [22] Otanicar TP, Phelan PE, Prasher RS, Rosengarten G, Taylor RA. Nanofluid-based direct absorption solar collect. *J Renew Sustain Energy* 2010;2(3).
- [23] Yousefi T, Veysi F, Shojaeizadeh E, Zinadini S. An experimental investigation on the effect of  $\text{Al}_2\text{O}_3$ - $\text{H}_2\text{O}$  nanofluid on the efficiency of flat-plate solar collector. *Renewable Energy* 2012;39:293–8.
- [24] Chaji H, Ajabshirchi Y, Esmaeilzadeh E, Zeinali Heris S, Hedayatzadeh M, Kahani M. Experimental study on thermal efficiency of flat plate solar collector using  $\text{TiO}_2$ /water nanofluid. *Modern Appl Sci* 2013;7:60–9.
- [25] Moghadam AJ, Farzane-Gord M, Sajadi M, Hoseyn-Zadeh M. Effects of  $\text{CuO}$ /water nanofluid on the efficiency of a flat plate solar collector. *Exp Therm Fluid Sci* 2014;58:9–14.
- [26] Colangelo G, Favale E, De Risi A, Laforgia D. A new solution for reduced sedimentation flat panel solar thermal collector using nanofluids. *Appl Energy* 2013;111:80–93.
- [27] EN 12975-2.
- [28] Fisher S, Heidemann W, Steinhagen HM, Perers B, Bergquist P, Hellström B. Collector test method under quasi-dynamic conditions according to the European Standard EN 12975-2. *Sol Energy* 2004;76:117–23.
- [29] Kebilinski P, Phillpot SR, Choi SUS, Eastman LA. Mechanisms of heat flow in suspensions of nano-sized particles (nanofluids). *Int J Heat Mass Transfer* 2000;45:855–63.
- [30] Jang SP, Choi SUS. Effects of various parameters on nanofluids thermal conductivity. *J Heat Transfer* 2007;129(May):617–23.
- [31] Xuan Y, Li Q. Investigation in convective heat transfer and flow features of nanofluids. *J Heat Transfer* 2003;125(February):151–5.